

# Nonequilibrium stationary states with ratchet effect

G. Cristadoro<sup>(a),(b)</sup> and D.L. Shepelyansky<sup>(b)\*</sup>

<sup>(a)</sup> *Center for Nonlinear and Complex Systems, Dipartimento di Scienze Chimiche, Fisiche e Matematiche, Università dell'Insubria, Via Valleggio 11, and Istituto Nazionale di Fisica della Materia, Unità di Como, 22100 Como, Italy*

<sup>(b)</sup> *Laboratoire de Physique Théorique, UMR 5152 du CNRS, Université P. Sabatier, 31062 Toulouse Cedex 4, France*

(Dated: October 20, 2004)

An ensemble of particles in thermal equilibrium at temperature  $T$ , modeled by Nosè-Hoover dynamics, moves on a triangular lattice of oriented semi-disk elastic scatterers. Despite the scatterer asymmetry a directed transport is clearly ruled out by the second law of thermodynamics. Introduction of a polarized zero mean monochromatic field creates a directed stationary flow with nontrivial dependence on temperature and field parameters. We give a theoretical estimate of directed current induced by a microwave field in an antidot superlattice in semiconductor heterostructures.

PACS numbers: 05.70.Ln, 05.45.Pq, 72.40.+w

According to the second law of thermodynamics there is no stationary directed transport in spatially periodic asymmetric systems in thermal equilibrium [1, 2]. However, a time periodic parameter variation may drive such a system out of equilibrium leading to the emergence of stationary transport whose direction depends non trivially on parameters. Such directed transport appears in systems with noise, fluctuations and dissipation and is now called Brownian motor or ratchet (see e.g. reviews [3, 4, 5]). The ratchet effect has a generic nature and it has been observed in various physical systems including semiconductor heterostructures [6], cold atoms in a laser field [7], vortices in superconductors [8, 9, 10] and macroporous silicon membranes under pressure oscillations [11]. It has also important applications in biological systems as discussed in [4, 12].

In spite of a great recent interest to ratchets the theoretical research is mainly concentrated on one-dimensional models (see e.g. [5]). Also, since the ratchet behavior is usually rather complex, an overdamped limit is used very often to obtain analytical parameter dependence even if in this regime a directed transport is absent for  $ac$  zero mean force [5]. To understand in a better way the global properties of ratchets and their dependence on such important physical parameters as temperature  $T$  and driving strength  $\mathbf{f}$ , we analyze here a generic case when  $ac$ -driving affects a Maxwell thermostat ensemble of noninteracting particles moving in an asymmetric two-dimensional (2D) periodic structure. This structure is composed of triangular 2D-lattice of rigid semi-disks of radius  $r_d$  as shown in Fig. 1 (insert). The distance  $R$  between disk centers is fixed to be  $R = 2r_d$  and we assume that collisions with semi-disks are elastic. Free particle motion between semi-disks is affected by a polarized monochromatic force  $\mathbf{f} = f(\cos\theta, \sin\theta)\cos\omega t$  with frequency  $\omega$ , strength  $f$  and polarization angle  $\theta$  to  $x$ -axis. It is also assumed that particles are in thermal equilibrium and at  $f = 0$  their velocities are given by

the Maxwell distribution at temperature  $T$ . Fig. 1 shows that in this system  $ac$ -force generates stationary directed transport. In the following we put  $r_d$ , particle mass  $m$ , unit of time and Boltzmann's constant  $k$  to be equal to unity.

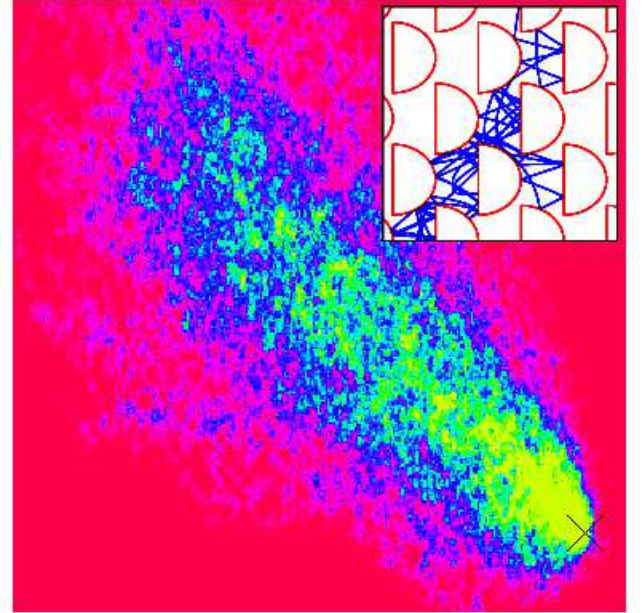


FIG. 1: (color online) Density distribution averaged over the time interval  $0 \leq t \leq 5 \cdot 10^5$  and obtained from dynamics of 200 particles given by the Nosè-Hoover equations at thermostat temperature  $T = 24$ . The region of distribution is  $x = [-2050, 150]$ ,  $y = [-300, 1900]$ . Initially particles are placed at  $x = y = 0$  (cross) with random velocities. Density is proportional to color changing from zero (red/black) to maximum (yellow/white). The parameters of driving force are  $f = 16$ ,  $\omega = 1.5$  and  $\theta = \pi/8$ . The relaxation time scale of the thermostat is  $\tau = \sqrt{50}$ . Insert shows one trajectory on small scale moving between semi-disks.

In order to put particles in thermal equilibrium we choose the elegant method of the Nosè-Hoover thermo-

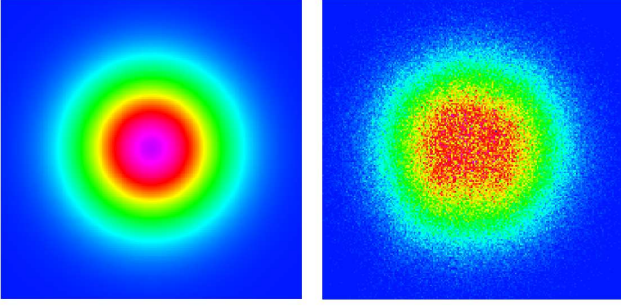


FIG. 2: (color online) Steady state distribution in 2D momentum plane  $(p_x, p_y)$ , density is proportional to color changing from zero (blue/black) to maximum (rose-violet/gray). Left: the Maxwell distribution at temperature of Fig. 1; right: distribution obtained numerically from the Nosé-Hoover thermostat for the case of Fig. 1.

stat (see e.g. [13, 14, 15] and Refs. therein). In this method the motion of a particle is affected by an effective friction  $\gamma$  which keeps the average kinetic energy  $\langle \mathbf{p}^2/2 \rangle$  equal to a given thermostat temperature  $T$ . In this way the dynamics of particle is described by the equations:

$$\dot{\mathbf{q}} = \mathbf{p}/m, \quad \dot{\mathbf{p}} = \mathbf{F} - \gamma \mathbf{p}, \quad \dot{\gamma} = [\mathbf{p}^2/(2T) - 1]/\tau^2 \quad (1)$$

where  $\mathbf{q}, \mathbf{p}$  are particle coordinate and momentum,  $\mathbf{F}$  is a sum of *ac*-force and force of elastic collisions with semi-disks, and  $\tau$  is the time scale of relaxation to equilibrium.

It is known that the Nosé-Hoover thermostat works well only if the dynamics is sufficiently chaotic [13, 14, 15]. In some cases, e.g. for the Galton board, the Nosé-Hoover thermostat gives noticeable deviations from the Maxwell distribution [15]. To check that in our case this method really gives a thermal equilibrium we analyze the steady state distribution in the momentum space obtained by numerical Runge-Kutta integration of Eqs.(1). Our results show that a small *ac*-force is needed to make chaotic dynamics between semi-disks more homogeneous and to produce a stable Maxwell thermal equilibrium which is not sensitive to variation of relaxation rate  $1/\tau$  (Fig.3, insert). At large force the numerical data show that 2D steady state in the momentum space is still close to the Maxwell distribution (Fig. 2) even if the *ac*-driving produces a clear ratchet effect shown in Fig. 1. The dependence of steady state on temperature closely follows the Maxwell distribution in momentum space  $p = |\mathbf{p}|$  as shown in Fig. 3. Thus we may conclude that the dynamics given by the Nosé-Hoover equations allows efficiently investigate the effects of *ac*-driving on particles in thermal equilibrium. The numerical data show that this driving generates a strong ratchet effect (Fig. 1) with directed transport depending of temperature and parameters of driving force.

To understand the properties of this directed transport we first analyze the dependence of averaged friction  $\langle \gamma \rangle$

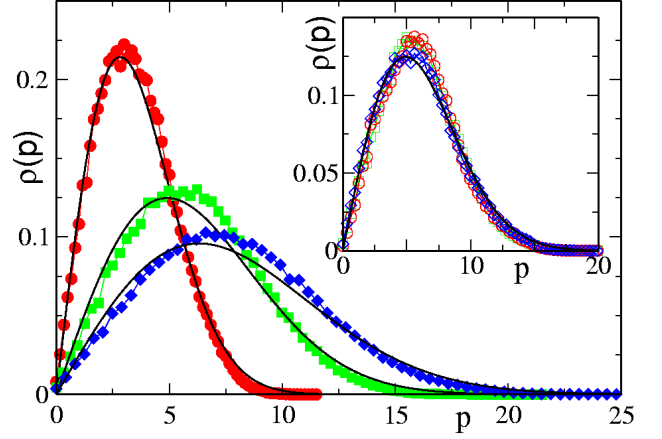


FIG. 3: (color online) Thermal distribution  $\rho$  in momentum  $p = |\mathbf{p}|$  for different values of temperature  $T = 8, 16, 40$  (from narrow to broad distribution, respectively, shown by curves and symbols). For each temperature value the curve gives the Maxwell distribution and the symbols show the numerical data for the Nosé-Hoover thermostat ( $\tau = \sqrt{50}$ ) in presence of *ac*-driving with parameters of Fig. 1. Insert shows the stability of Nosé-Hoover thermostat at small *ac*-force ( $f = 0.5, \omega = 1.5, \theta = \pi/8$ ) with respect to variation of relaxation time  $\tau^2 = 1$  (circles), 50 (squares), 100 (diamonds) at fixed temperature  $T = 24$ ; curve shows the Maxwell distribution. All numerical data are obtained from one long trajectory with  $t \leq 5 \cdot 10^5$ .

on driving strength  $f$  and temperature  $T$ . The value of  $\langle \gamma \rangle$  is obtained by averaging over long time interval during numerical integration of Eqs.(1) for one trajectory. We also checked that averaging over a few trajectories gives the same result. The data are shown in Fig. 4. They are well described by a global scaling given by [16]

$$\langle \gamma \rangle = C r_d f^2 / T^{3/2}. \quad (2)$$

Small deviations seen at low  $T$  appear because of strong driving force which starts to modify significantly the particle velocity distribution in this regime. The numerical constant  $C$  is only weakly dependent on  $\theta$  and  $\omega$  changing by 50% to 30% when  $\theta$  changes from 0 to  $\pi/2$  and  $\omega$  changes by a factor 10, respectively. The dependence (2) clearly tells that in presence of driving force the thermostat creates an effective friction force  $\mathbf{f}_f = -\langle \gamma \rangle \mathbf{p}$  acting on particle propagation with an effective friction constant  $\langle \gamma \rangle$ . Surprisingly, this friction coefficient varies with  $f$  and  $T$  according to Eq.(2) but in a large range remains independent of the relaxation time  $\tau$  (Fig. 4 insert). We note that the particle dynamics in absence of thermostat but in presence of friction force  $\mathbf{f}_f = -\gamma \mathbf{p}$  with constant friction coefficient  $\gamma$  has been analyzed in [17] where it was shown that *ac*-force generates a directed transport on semi-disk lattice.

To understand the origin of the dependence (2) we put forward the following heuristic arguments. The driving force gives a diffusive energy growth during a dissipative

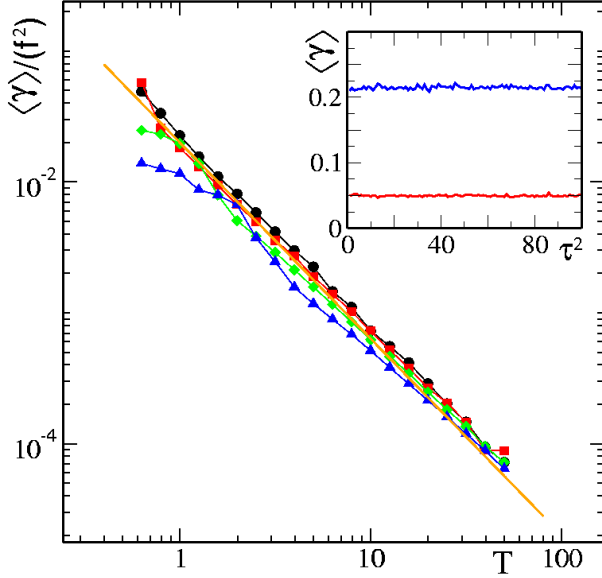


FIG. 4: (color online) Dependence of rescaled average friction coefficient  $\langle \gamma \rangle / f^2$  on temperature  $T$  for  $f = 4$  (circles), 8 (squares), 16 (diamonds), 32 (triangles) (top to bottom) at fixed  $\omega = 1.5$ ,  $\theta = 0$ ,  $\tau^2 = 50$ . The straight line shows dependence (2) with  $C = 0.02$ . Insert shows that  $\langle \gamma \rangle$  is robust against variation of  $\tau^2$  in the interval [1, 100] (with step 1); data are shown for  $f = 16$ ,  $\omega = 1.5$ ,  $\theta = 0$ ,  $T = 8$  (top curve) and 24 (bottom curve).

time scale  $1/\gamma$  so that

$$(\Delta E)^2 \sim D_E / \gamma, \quad D_E \sim f^2 v l, \quad (3)$$

where the diffusion rate in energy is  $D_E \sim \dot{E}^2 \tau_c \sim f^2 v l$  and the mean-free path  $l \sim R \sim r_d \sim 1$  determines the collision time  $\tau_c = l/v$ . In the Maxwell equilibrium the particle velocity is  $v \sim T^{1/2}$  and the fact that the driving force does not modify the velocity distribution implies that  $\Delta E \sim T$  so that the diffusive growth is stopped by effective friction  $\gamma \sim D_E / T^2 \sim r_d f^2 / T^{3/2}$  in agreement with (2). In fact there is a close relation to results [17] where the thermostat is absent but a friction force  $\mathbf{f}_f = -\gamma \mathbf{p}$  with constant  $\gamma$  affects particle dynamics. There *ac*-driving heats a particle up to energy  $E \sim (r_d f^2 / \gamma)^{2/3}$  while in presence of thermostat the energy is fixed by temperature  $T \sim E$  that imposes a convergence to the stationary state with effective friction given by (2) [18].

The dependence of average velocity  $v_f$  of the ratchet flow on  $\langle \gamma \rangle$  for various values of driving strength  $f$  is shown in Fig. 5. Globally, the flow velocity  $v_f$  grows with increase of  $\gamma$ . Two regimes are clearly seen:  $v_f \approx \langle \gamma \rangle$  for  $\langle \gamma \rangle < \gamma_c$  and  $v_f \approx (f \langle \gamma \rangle)^{1/3} / 10$  for  $\langle \gamma \rangle > \gamma_c \approx f^{1/2} / 30$ . In fact this dependence is very close to the one found in a model with fixed  $\gamma$  [17]. As a result, from (2) we obtain the dependence of flow velocity on temperature:

$$v_f / v \approx r_d f / 50 T, \quad (T < T_c); \quad (4)$$

$$v_f / v \approx (r_d f / 8 T)^2, \quad (T > T_c); \quad (5)$$

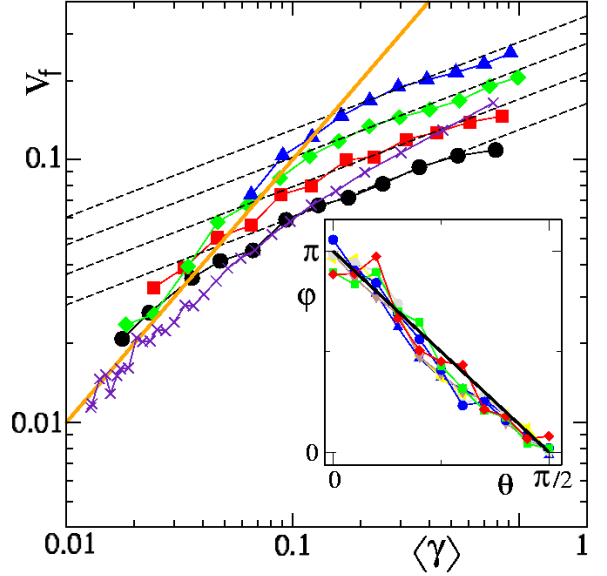


FIG. 5: (color online) Dependence of the absolute value of average velocity of particle flow  $v_f$  on average friction  $\langle \gamma \rangle$  for the parameters of Fig. 4 with  $f = 4, 8, 16, 32$  (same symbols, from bottom to top). Dashed lines show the scaling dependence  $v_f \sim (f \langle \gamma \rangle)^{1/3}$  at large  $\langle \gamma \rangle$  for different  $f$  values; the full line shows scaling  $v_f = \langle \gamma \rangle$  at small  $\langle \gamma \rangle$ . Crosses show data for the same parameters as for squares ( $f = 8$ ) but with additional circular scatterer added in the center of unit cell to eliminate orbits with a straight flight through the whole system (see text). Insert shows the dependence of flow direction angle  $\varphi$  on polarization angle  $\theta$ ; data are given for  $f = 8$ ,  $\omega = 1.5$ ,  $\tau^2 = 50$  and  $4 \leq T \leq 11$ ; full line shows average dependence  $\varphi = \pi - 2\theta$ .

where  $v = (2T)^{1/2}$  is the thermal velocity and  $T_c \approx r_d f$  is linked to  $\gamma_c$  obtained from Fig. 5. The transition between two regimes takes place when the energy given by *ac*-force to particle between two collisions becomes larger than temperature ( $T < T_c$ ). In that case the effect of driving is strong and  $v_f \sim f \tau_c \sim r_d f / T^{1/2}$  leading to (4). For  $T > T_c$  thermal fluctuations are strong and the ratchet effect appears only in the second order of force  $f$  giving (5). The numerical factors in (4),(5) are taken for the case  $\theta = 0$  from Figs. 4,5. We note that Eqs. (2)-(5) are derived in the regime of relatively weak friction  $\langle \gamma \rangle \ll \omega$  and relaxation rate  $1/\tau \ll \omega$ . Another important point is that the dependence (4),(5) is robust with respect to variation of scatterer geometry, e.g. introduction of additional disk scatterer in the center of unit cell eliminates all collisionless paths but gives no significant modifications (see Fig. 5).

The dependence of flow directionality, determined through angle  $\varphi$  ( $\mathbf{v}_f = v_f(\cos \varphi, \sin \varphi)$ ), on the polarization of *ac*-force is shown in Fig. 5 (insert). In average, it is satisfactorily described by the relation  $\varphi = \pi - 2\theta$  (similar dependence was seen in [17]). On a qualitative ground, we may say that at  $\theta = 0$  due to friction a particle

becomes trapped between semi-disks of a unit cell that gives a directed transport to the left while for  $\theta = \pi/2$  vertical oscillations push particle to the right in presence of friction. The linear dependence  $\varphi = \pi - 2\theta$  interpolates between these two limits. However, a more quantitative derivation is needed.

It is interesting to apply the approach developed above to other types of thermostat. It is possible to realize the semi-disk Galton board with antidot superlattices for 2D electron gas in semiconductor heterostructures. With such structures the Galton board of disks has already been implemented (see e.g. [19]) and effects of microwave radiation has been studied [20]. For disk antidots like those in [19, 20] the ratchet effect is absent due to symmetry of antidot. However, for semi-disk antidot lattice strong ratchet effect should appear. To find its properties we should take into account that in this case we have the Fermi-Dirac thermostat with the Fermi energy  $E_F \gg T$ . Due to that in (3) the particle velocity  $v$  is equal to the Fermi velocity  $v_F = (2E_F/m)^{1/2}$  independent of  $T$ . This modification gives the average friction  $\gamma_F$  for the Fermi gas

$$\gamma_F = Cf^2 v_F r_d / T^2 \approx v_f / r_d, \quad (6)$$

where we kept the same numerical constant  $C \sim 1/50$ . In fact (6) follows from  $D_E \sim f^2 v_F r_d$  (see (3)) and  $\gamma_F \sim D_E / T^2$ . The second equality in (6) appears due to the fact that  $E_F \gg T_c$  implying the regime (5) with  $v_f \sim \gamma_F r_d$ . Of course, only a small fraction  $T/E_F$  of electrons near  $E_F$  contributes to this ratchet flow. Hence, the current  $I$  per one semi-disk row is

$$I \sim e r_d n_e v_f T / E_F \sim C e r_d^3 \sqrt{n_e} f^2 / (T \hbar). \quad (7)$$

where we used that for the 2D electron Fermi gas  $E_F = \pi n_e \hbar^2 / m$ . We note that in semiconductor antidot lattices like in [19, 20] the effective mass  $m$  is about 15 times smaller compared to the electron mass. For a typical parameters of semi-disk antidot lattice with electron density  $n_e \sim 10^{12} \text{ cm}^{-2}$ ,  $r_d \sim 1 \mu\text{m}$ , field strength per electron charge  $f/e \sim 1 \text{ V/cm}$  and  $T \sim 10 \text{ K}$  we obtain  $v_f/v_F \sim 10^{-4}$ . At these parameters  $E_F \sim 150 \text{ K}$ ,  $v_F \sim 3 \cdot 10^7 \text{ cm/sec}$  and the current  $I \sim 10^{-9} \text{ A}$  is sufficiently large to be observed experimentally. The result (7) is based on the semiclassical estimate for the diffusion rate  $D_E$  which assumes that the energy of microwave photon is larger than the level spacing  $\Delta$  inside one unit cell:  $\hbar\omega > \Delta \approx 2\pi\hbar^2/(mr_d^2)$ . In the opposite limit  $\hbar\omega \ll \Delta$ ,  $ac$ -driving is in the quantum adiabatic regime when the excitation in energy is very weak. Thus for  $r_d \sim 1 \mu\text{m}$  we have  $\Delta \approx 5 \cdot 10^{-6} \text{ eV} \approx 0.05 \text{ K}$  and the directed transport appears only for  $\omega/2\pi > 1 \text{ GHz}$ . In experiments [6] the frequency was deeply in the adiabatic regime with  $\omega/2\pi \sim 100 \text{ Hz}$  and the directed transport was absent at zero mean force.

In summary, we showed that zero mean  $ac$ -force applied to particles being in thermal equilibrium in asymmetric periodic potential creates a directed transport flow. Its direction is efficiently changed by polarization of the force. We also established the dependence of the flow velocity  $v_f$  on temperature and driving field strength for the Maxwell [Eqs. (4),(5),(6)] and the Fermi-Dirac [Eqs. (6),(7)] thermostats.

We thank Alexei Chepelianskii, Kvon Ze Don and Sergey Vitkalov for useful discussions.

---

\* <http://www.lpt.irsamc.ups-tlse.fr/~dima>

- [1] M. v. Smoluchowski, *Physik. Zeitschr.* **13**, 1069 (1912).
- [2] R.P.Feynman, R.B.Leighton, and M.Sands, *The Feynman Lectures on Physics*, **1**, chapter 46, Addison Wesley, Reading MA (1963).
- [3] V.I.Belinicher, and B.I.Sturman, *Sov. Phys. Usp.* **23**, 199 (1980).
- [4] R.D. Astumian and P. Hänggi, *Physics Today* **55** (11), 33 (2002).
- [5] P. Reimann, *Phys. Rep.* **361**, 57 (2002).
- [6] H. Linke, T.E. Humphrey, A. Löfgren, A.O. Sushkov, R. Newbury, R.P. Taylor, and P. Omling, *Science* **286**, 2314 (1999).
- [7] C. Mennerat-Robilliard, D. Lucas, S. Guibal, J. Tabosa, C. Jurczak, J.-Y. Courtois, and G. Grynberg, *Phys. Rev. Lett.* **82**, 851 (1999).
- [8] J.B. Majer, J. Peguiron, M. Grifoni, M. Tusveld, and J.E. Mooij, *Phys. Rev. Lett.* **90**, 056802 (2003).
- [9] J.E. Villegas, S. Savel'ev, F. Nori, E.M. Gonzalez, J.V. Anguita, R. Garcia, and J.L. Vicent, *Science* **302**, 1188 (2003).
- [10] A.V. Ustinov, C. Coqui, A. Kemp, Y. Zolotaryuk and M. Salerno, *Phys. Rev. Lett.* **93**, 087001 (2004).
- [11] S. Matthias and F. Müller, *Nature* **424**, 53 (2003).
- [12] F. Jülicher, A. Ajdari, and J. Prost, *Rev. Mod. Phys.* **69**, 1269 (1997).
- [13] W. G. Hoover, *Phys. Rev. A* **31**, 1695 (1985).
- [14] W. G. Hoover, *Time reversibility, computer simulation, and chaos*, World Scientific, Singapore (1999).
- [15] K. Rateitschak, R. Klages, W. G. Hoover, *J. Stat. Phys.* **101**, 61 (2000).
- [16] To mark the right dimension we keep in formulas  $r_d = 1$  but omit  $m = 1$  which is easy to restore.
- [17] A. D. Chepelianskii and D. L. Shepelyansky, *cond-mat/0402675*.
- [18] We note that a numerical constant  $C \approx 0.02$  in (2) (see Fig. 4) corresponds to average dependence  $v^2 = 2T = (f^2/\gamma)^{2/3}/7$  from Fig. 5 in [17].
- [19] D. Weiss, M. L. Roukes, A. Menschig, P. Grambow, K. von Klitzing, and G. Weimann, *Phys. Rev. Lett.* **66**, 2790 (1991).
- [20] A.A. Bykov, G.M. Gusev, Z.D.Kvon, V.M.Kudryashev, and V.G.Plyukhin, *Pis'ma Zh. Eksp. Teor. Fiz.* **53**, 407 (1991) [*JETP Lett.* **53**, 427 (1991)].